GMV: A Unified and Efficient Graph Multi-View Learning Framework

Qipeng Zhu[1]*, **Jie Chen**[2]*, **Jian Pu**[3]†, **Junping Zhang**[1]†
[1]Shanghai Key Laboratory of Intelligent Information Processing,
College of Computer Science and Artificial Intelligence, Fudan University
[2] College of Computer and Data Science, Fuzhou University
[3]Institute of Science and Technology for Brain-Inspired Intelligence, Fudan University
qpzhu23@m.fudan.edu.cn, jiechen202@fzu.edu.cn,
{jpzhang,jianpu}@fudan.edu.cn

Abstract

Graph Neural Networks (GNNs) are pivotal in graph classification but often struggle with generalization and overfitting. We introduce a unified and efficient Graph Multi-View (GMV) learning framework that integrates multi-view learning into GNNs to enhance robustness and efficiency. Leveraging the lottery ticket hypothesis, GMV activates diverse sub-networks within a single GNN through a novel training pipeline, which includes mixed-view generation, and multi-view decomposition and learning. This approach simultaneously broadens "views" from the data, model, and optimization perspectives during training to enhance the generalization capabilities of GNNs. During inference, GMV only incorporates additional prediction heads into standard GNNs, thereby achieving multi-view learning at minimal cost. Our experiments demonstrate that GMV surpasses other augmentation and ensemble techniques for GNNs and Graph Transformers across various graph classification scenarios. The open source code can be found in https://github.com/smurf-1119/GMV.

1 Introduction

Graph Neural Networks (GNNs) have emerged as a powerful tool for graph classification tasks, attracting considerable attention. Despite their success, GNNs struggle with generalization and overfitting due to the complex nature of graph structures and the limited availability of labeled graph data [1, 2]. As shown in Fig 1, simply increasing the parameters of GNNs does not consistently enhance their performance [3]. A promising solution lies in multi-view learning, which enables models to extract diverse representations by aggregating complementary perspectives of data [4, 5]. By forcing models to reconcile differences across views, multi-view learning offers a fundamental insight of diversity for enhancing model generalization.

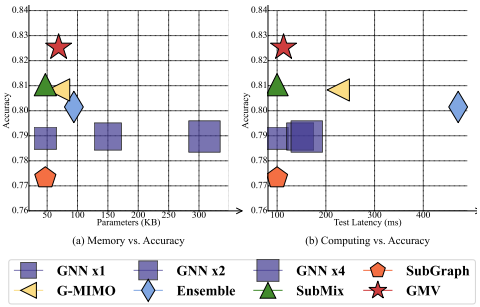

Figure 1: Accuracy vs. memory/speed. Specifically, "GNN x$*$" represent different sizes of GNNs.

*Qipeng Zhu and Jie Chen are co-first authors.
†Junping Zhang and Jian Pu are corresponding authors.

39th Conference on Neural Information Processing Systems (NeurIPS 2025).

Existing graph learning strategies implicitly leverage multi-view principles but remain suboptimal. Graph data augmentation (e.g., DropEdge [6], S-Mixup [7]) diversifies input views via edge removal or graph interpolation, acting as "data-view" expansions. However, these methods often degrade structural integrity (e.g., random edge dropping disrupts critical topological hierarchies [8]), limiting their effectiveness on structured graphs. Ensemble learning [9, 10, 11] achieves "model-view" diversity by training multiple GNNs, but at the cost of significant computational overhead as illustrated in Fig 1. The need for separate forward passes across networks renders these methods infeasible for large graphs. These strategies treat data and model views in isolation, failing to exploit the synergistic power of multi-view learning.

In this paper, we introduce a unified and efficient **G**raph **M**ulti-**V**iew (GMV) learning framework. GMV is model-agnostic and expands views from three complementary perspectives—data, model, and optimization—to activate diverse sub-networks within a single GNN. Inspired by the lottery ticket hypothesis [12], where neural networks contain latent sub-networks with comparable performance to the full model, we aim to overcome the challenge that standard supervised training fails to activate such diversity [13, 4]. Specifically, we design a novel training pipeline integrating mixed-view generation and multi-view decomposition and learning.

During training, GMV employs a three-fold coherent strategy to unify multi-view learning. *From a data perspective*, we propose structure enhanced subgraph mixing, which samples two subgraphs that preserve both the topological structure and semantic nodes to generate mixed graph views. This mixed view contains the multi-view knowledge and addresses the structural loss in prior augmentations. *From a model perspective*, we introduce a lightweight dual-output prediction head to explicitly activate two sub-networks within any single GNN and Graph Transformer (GT). This design enables parallel encoding of mixed views and multi-view decomposition in one forward pass, eliminating the multi-model overhead of ensemble methods while preserving representation diversity. *From a optimization perspective*, we design multi-view and mixed-view loss functions. These two losses collectively supervise view-specific predictions and activate sub-networks to learn diverse multi-view representations. During inference, GMV processes standard graph input and simply averages dual-head outputs with single-model efficiency. By unifying data, model, and optimization perspectives of multi-view learning, GMV provides a generalizable solution for GNNs and GTs. As illustrated in Fig 1, GMV achieves the best trade-off between overhead and accuracy.

Our contribution can be summarized as follows: 1) We introduce GMV, a unified and efficient multi-view learning framework that enhances the robustness and generalization of both GNNs and GTs in graph classification tasks. 2) We propose new structure-enhanced subgraph mixing techniques, accompanied by multi-view and mixed-view loss, to encourage models to learn from diverse graph views. 3) Our comprehensive experiments evaluate the efficacy, robustness, and generalization of GMV. GMV significantly improves GNNs/GTs and achieves state-of-the-art results compared to various graph augmentation and graph ensembling methods.

2 Related Work

Graph Neural Network. Graph Neural Networks (GNNs) leverage the message passing mechanism [14, 15] to aggregate and update node representations for graph data processing [16, 17, 18]. The Graph Convolutional Network (GCN) [19] uniformly aggregates neighbor messages to update node embeddings. GraphSAGE [20] introduces subgraph sampling with diverse aggregation methods for adaptive representations. The Graph Isomorphism Network (GIN) [21] further refines this by capturing graph isomorphism, enhancing model sensitivity to graph topology. Moreover, combining the GNN with transformer architecture, such as Graphomer [22] and GraphGPS [23], has also emerged in graph learning fields.

Multi-view Learning. In computer vision, multi-view data, typically derived from various perspectives with shared high-level semantics, has become a crucial data type [24]. Asif et al. [4] apply multi-view learning theory to multi-class classification, suggesting that each image has an inherent "multi-view" structure, where these "multi-view" structures correspond to multiple data features that can help deep neural networks in accurate classification. They demonstrate how multi-view learning can improve both the generalization and robustness of deep neural networks. While several multi-view learning strategies [25, 26, 27, 28, 29] have been proposed for graph tasks, their application to supervised graph classification remains challenging due to differences in task objectives

and data characteristics. For example, Yuan et al. [27] generate node feature views for both labeled and unlabeled nodes in node classification, whereas Liu et al. [28] generate views based on pairs of positive and unlabeled graphs in graph classification. Both focus on semi-supervised learning. Compared to image classification, generating mixed-views that preserve both structural and semantic information in graph classification is more difficult. In this paper, we propose generating mixed-views to activate dual sub-networks within GNNs, enhancing multi-view learning capabilities from the data, model, and optimization perspectives.

Graph Augmentation. We conceptualize graph augmentation as a specialized form of multi-view learning, aimed at expanding graph datasets through modifications. One approach involves randomly modifying the original graph while assuming the label remains unchanged, such as DropNode [30], DropEdge [6], and Subgraph [31]. However, the simplicity of these operations often limits the diversity of the resulting graph views and may introduce noise. Other approaches integrate mixup techniques [32] into graph classification. For example, S-Mixup [7] aligns pairs of graphs using a soft alignment matrix derived from a trained Graph Matching Network (GMN), followed by linear interpolation of the aligned graphs. Nevertheless, the complexity and resource demands of training an effective GMN often lead to suboptimal performance due to inadequate mapping. Techniques like SubMix [33] and GraphTransplant [34] connect subgraphs sampled from different graphs to facilitate model-agnostic graph augmentation. However, these methods do not fully exploit the sub-views of graphs and often neglect structural information. In contrast, GMV effectively integrates structure-enhanced sub-views to generate mixed views, while utilizing a multi-view decomposition and learning pipeline to extract diverse view representations.

Ensemble Learning. Ensemble learning [9, 4, 35] aims to improve the robustness and generalization of a single model by combining the outputs of multiple models. This approach, however, comes with high computational and memory demands. The Lottery Ticket Hypothesis [12, 36] posits that dense neural networks contain sparse subnetworks ("winning tickets") capable of achieving comparable performance when trained in isolation, which suggests the possibility of ensemble learning with these subnetworks. In the realm of image classification, MIMO [13] introduces multi-input multi-output techniques to ensemble sub-networks within a single convolutional neural network. Despite these advancements, applying ensemble learning effectively to Graph Neural Networks (GNNs) remains a challenge, primarily due to the arbitrary sizes of graphs. G-MIMO [37] addresses this by implementing graph multi-input and multi-output schemes, adding multiple parallel graph encoders and decoders. However, this approach complicates the forward passing process in GNNs and struggles with limited graph views. In contrast, our proposed method, GMV, minimizes transformations for GNNs and achieves efficient ensembling through a single forward pass, efficiently enhancing the multi-view learning capability.

3 Method

To enhance the robustness and generalization of GNNs through multi-view graph learning, we simultaneously increase the diversity of input graph views and the multi-view learning capabilities of GNNs. As illustrated in Figure 2, we first outline the process of mixed-view generation. Then, we introduce details of mixed-view decomposition and multi-view learning, which activate dual sub-networks within a single GNN for efficient ensemble.

3.1 Preliminaries

An undirected graph $\mathcal{G} =< \mathcal{V}, \mathcal{E}, \mathbf{A}, \mathbf{X} >$, where $\mathcal{V} = \{v_i | 1 \leq i \leq n\}$ represents the set of nodes, and $\mathcal{E} = \{e_{ij} | v_i \in \mathcal{V} \wedge v_j \in \mathcal{V} \wedge v_i \text{ is connected to } v_j\}$ is the set of edges. The matrix $\mathbf{X} \in \mathbb{R}^{n \times d}$ contains the node features, while $\mathbf{A} \in \{0, 1\}^{n \times n}$ is the adjacency matrix where $\mathbf{A}_{ij} = 1$ if nodes v_i and v_j are connected. The degree matrix $\mathbf{D} \in \mathbb{R}^{n \times n}$ has entries $\mathbf{D}_{ii} = \sum_j \mathbf{A}_{ij}$ on the diagonal, with $\mathbf{D}_{ij} = 0$ for $i \neq j$. Each node $v_i \in \mathcal{V}$ has a neighborhood set, denoted $\mathcal{N}(v_i) = \{v_j | v_i \text{ is connected to } v_j \wedge v_j \in \mathcal{V}\}$. For graph classification, a collection of n undirected graphs is represented as $\mathbb{G} = \{(\mathcal{G}_t, \mathbf{y}_t)\}_{t=1}^{n}$, where $\mathbf{y}_t \in \{0, 1, \ldots, C-1\}$ denotes the label for each graph $\mathcal{G}_t$, and C is the number of classes.

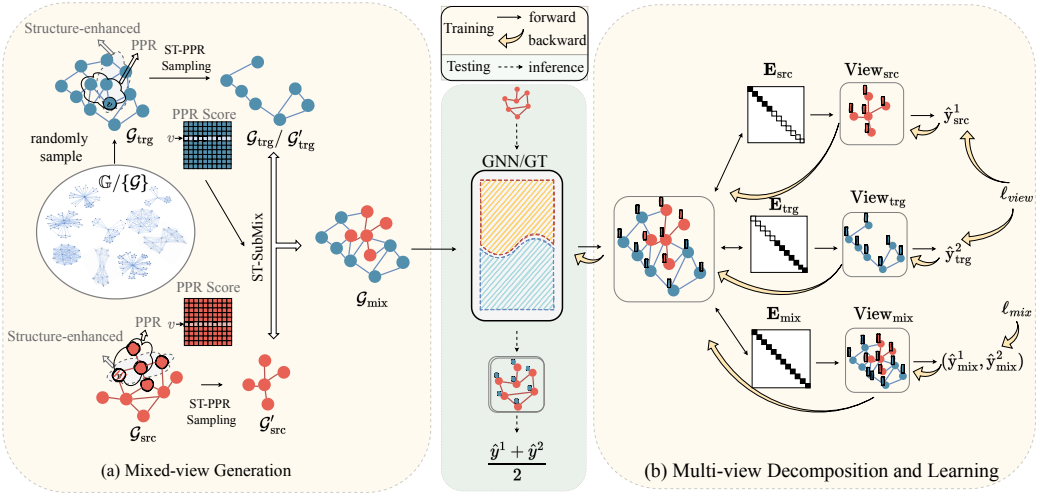

Figure 2: (a) For data perspective, GMV connects two structure enhanced subgraphs to generate the mixed-view. (b) For model perspective, GMV employs dual sub-networks in GNN/GT to gain diverse view representations, denoted as multi-view decomposition. For optimization perspective, we design the multi-view learning process with multi-view (ℓ_{view}) and mixed-view loss (ℓ_{mix}) to optimize dual sub-networks. When testing, GMV simply averages two predictions of dual sub-networks in GNN/GT as the final output.

3.2 Mixed-view Generation

From a data perspective, we explore how to integrate diverse views from different graphs into a single graph, allowing the GNN to process them concurrently and activating sub-networks to learn multi-view representations. Unlike previous graph augmentations [6, 7, 31], our method explicitly considers the critical structural information [38] to generate a mixed graph view. This is achieved through a structure-enhanced subgraph sampling, followed by structure-enhanced subgraph mixing.

3.2.1 Structure Enhanced Subgraph Sampling

Unlike random corruption of graphs [6, 30], sampling subgraphs preserves more semantic information [39]. We employ subgraph sampling methods to construct richer views. A key challenge is exploring various subgraphs that encapsulate the most crucial semantic and structural information. Compared to randomly sampling [40], subgraph sampling methods based on Personalized PageRank (PPR) [41] and Determinantal Point Processes (DPP) [42, 43] can enhance the performance of GNNs without altering their architectures. However, the PPR-based method does not explicitly preserve the structure of the original graph, while the DPP-based method may overlook some key nodes due to its limited search scope. Considering that topology information effectively preserves label information during subgraph sampling [44], we propose a novel **ST**ructure Enhanced **PPR** subgraph sampling method (**ST-PPR**), which considers both key nodes and structural information.

The specific process is outlined in Algorithm 1. We first pick a random root node v from the graph $\mathcal{G}$. We consider both structural and semantic information of $\mathcal{G}$ by merging different node candidate sets [44]. Depth-First-Search (DFS) algorithm and Breath-First-Search (BFS) algorithm [45] can easily extract the original topology structure of $\mathcal{G}$. And the PPR algorithm considers semantic information by iteratively calculating the importance score of every node in $\mathcal{G}$ [33]. Therefore, we respectively use DFS, BFS and PPR methods to gain sampling node set $\{\mathcal{V}_{\text{BFS}}, \mathcal{V}_{\text{DFS}}, \mathcal{V}_{\text{PPR}}\}$ from $\mathcal{G}$. We set w as the maximum searching steps for DFS and BFS algorithms. To preserve those important nodes, we calculate the affinity personalized pagerank score matrix $\mathbf{S}_{\text{PPR}}$ [41] as follows:

$$\mathbf{S}_{\text{PPR}} = \sum_{r=0}^{\infty} \beta(1-\beta)^r \left(\mathbf{D}^{-1/2}(\mathbf{A}+\mathbf{I})\mathbf{D}^{-1/2}\right)^r, \tag{1}$$

where $\mathbf{D}$ and $\mathbf{A}$ respectively is the degree matrix and the adjancy matrix of $\mathcal{G}$ and $\mathbf{I}$ is the identity matrix. We set teleport probability β as 0.15 and affinity scores of nodes with respect to node v

are contained in $\mathbf{S}_{\text{PPR}}[:, v]$. Then we sort nodes in $\mathcal{V}$ following the scores $\mathbf{S}_{\text{PPR}}[:, v]$ and select top s_{PPR} nodes to get the node set $\mathcal{V}'_{\text{PPR}}$. And $\mathcal{V}'_{\text{BFS}}$ and $\mathcal{V}'_{\text{DFS}}$ both contain s_2 nodes respectively sampled from $\mathcal{V}_{\text{DFS}}$ and $\mathcal{V}_{\text{BFS}}$. We merge three node sets $\{\mathcal{V}'_{\text{PPR}}, \mathcal{V}'_{\text{DFS}}, \mathcal{V}'_{\text{BFS}}\}$ and reorder nodes by $\mathbf{S}_{\text{PPR}}[:, v]$ to obtain $\mathcal{V}'$.

Algorithm 1 Structure Enhanced PPR Subgraph Sampling

Input: Graph $\mathcal{G} =< \mathcal{V}, \mathcal{E}, \mathbf{A}, \mathbf{X} >$, augmentation ratio of $p \in (0, 1)$, structure augmentation ratio of q, number of walks w
Output: Ordered node set $\mathcal{V}'$

$v \leftarrow$ pick a random root node from $\mathcal{G}$.
$s_{\text{PPR}} \leftarrow$ sample size is $\max\{\mathbb{U}(0, p) \cdot |\mathcal{G}| - q, 0\}$
$s_2 \leftarrow$ sample size is $\lfloor (p \cdot |\mathcal{G}| - s_{\text{PPR}})/2 \rfloor$
$\mathbf{S}_{\text{PPR}} \leftarrow$ compute score by PPR$(\mathcal{G}, r)$
$\mathcal{V}_{\text{PPR}} \leftarrow$ Sort$(\mathcal{V}, \mathbf{S}_{\text{PPR}}[:, v])$, $\mathcal{V}'_{\text{PPR}} \leftarrow \mathcal{V}_{\text{PPR}}[: s_{\text{PPR}}]$
$\mathcal{V}_{\text{DFS}} \leftarrow$ DFS$(\mathcal{G}, v, w)$, $\mathcal{V}'_{\text{DFS}} \leftarrow$ Sample$(\mathcal{V}_{\text{DFS}}, s_2)$
$\mathcal{V}_{\text{BFS}} \leftarrow$ BFS$(\mathcal{G}, v, w)$, $\mathcal{V}'_{\text{BFS}} \leftarrow$ Sample$(\mathcal{V}_{\text{BFS}}, s_2)$
$\mathcal{V}' \leftarrow$ merge $\{\mathcal{V}'_{\text{PPR}}, \mathcal{V}'_{\text{DFS}}, \mathcal{V}'_{\text{BFS}}\}$ and sort them by $\mathbf{S}_{\text{PPR}}$

Combining PPR, BFS, and DFS, the sampled subgraphs covers global hubs, local communities, and long-range paths. This ensures comprehensive feature extraction including global topology , hierarchical transitions and local communities, which boosts the performance of GNNs. The proof is stated in Appendix 6.1.

3.2.2 Structure Enhanced Subgraph Mixing

To enable GNNs to effectively process diverse views simultaneously for multi-view learning, we integrate these views of diverse sub-graphs into a single mixed-graph. Inspired by SubMix [33], we propose a **ST**ructure-enhanced **Sub**graph **Mix**ing method (ST-SubMix), which connects two subgraphs according to a node mapping algorithm based on $\mathbf{S}_{\text{PPR}}$. Compared to SubMix, ST-SubMix connects two structure-enhanced subgraph views, thereby preserving more structure and label information from original graphs. The specific process is detailed in Algorithm 2.

Given a source graph (a primary training sample within a given batch), $\mathcal{G}_{\text{src}}$, we randomly sample a target graph (another graph from the same training batch), $\mathcal{G}_{\text{trg}}$ from $\mathbb{G}/\{\mathcal{G}_{\text{src}}\}$. We connect two subgraphs sampled from them to generate $\mathcal{G}_{\text{mix}}$. According to Algorithm 1, we gain $\mathcal{V}'_{\text{src}}$ and $\mathcal{V}'_{\text{trg}}$ respectively sampled from $\mathcal{V}_{\text{src}}$ and $\mathcal{V}_{\text{trg}}$. To ensure the equality of sizes between $\mathcal{V}'_{\text{src}}$ and $\mathcal{V}'_{\text{trg}}$, we let $s = \min\{\mathcal{V}_{\text{src}}, \mathcal{V}_{\text{trg}}\}$. To efficiently mapping two node sets, we make the one-to-one mapping from $\mathcal{V}'_{\text{src}}$ to $\mathcal{V}'_{\text{trg}}$. As shown in Fig 2, we connect $\mathcal{G}'_{\text{src}}$ and $\mathcal{G}_{\text{trg}}/\mathcal{G}'_{\text{trg}}$, which ensures the size distribution of graphs keeping the same as the original distribution [33]. Specifically, we replace the subgraph $\mathcal{G}'_{\text{src}}$ in the graph $\mathcal{G}_{\text{src}}$ with the subgraph $\mathcal{G}'_{\text{trg}}$. To represent the label of the mixed-view, we calculate the confidence of labels of two graphs. As described in Equation (2), the confidence is measured by the count of edge sets within it:

$$w_{\text{src}} = 1 - |\mathcal{E}'_{\text{trg}}|/|\mathcal{E}_{\text{mix}}|, w_{\text{trg}} = |\mathcal{E}'_{\text{trg}}|/|\mathcal{E}_{\text{mix}}|. \tag{2}$$

The procedure in Algorithm 1 outlines a subgraph interpolation method for graph augmentation. It first establishes a canonical node correspondence between a source ($\mathcal{G}_{\text{src}}$) and target ($\mathcal{G}_{\text{trg}}$) graph by ordering their respective nodes via Personalized PageRank (PPR) scores, following the SubMix methodology. This alignment guides the replacement of a target subgraph with its source counterpart to generate a mixed-view graph. For downstream representation decomposition, two binary assignment matrices, $\mathbf{E}$src and $\mathbf{E}$trg, are constructed. Each row is a one-hot vector indicating if a node in the mixed graph originates from the source or target. The property $\mathbf{I} = \mathbf{E}_{\text{src}} + \mathbf{E}_{\text{trg}}$ ensures a disjoint partition of the node set, which is used to separate the view-specific representations from the mixed-view output.

Algorithm 2 Structure Enhanced Subgraph Mixing

Input: Graph $\mathcal{G}_{\text{src}} =< \mathcal{V}_{\text{src}}, \mathcal{E}_{\text{src}}, \mathbf{A}_{\text{src}}, \mathbf{X}_{\text{src}} >$, Graph $\mathcal{G}_{\text{trg}} =< \mathcal{V}_{\text{trg}}, \mathcal{E}_{\text{trg}}, \mathbf{A}_{\text{trg}}, \mathbf{X}_{\text{trg}} >$
Output: Mixed graph $\mathcal{G}_{\text{mix}} =< \mathcal{V}_{\text{mix}}, \mathcal{E}_{\text{mix}}, \mathbf{A}_{\text{mix}}, \mathbf{X}_{\text{mix}} >$, assignment matrices $\mathbf{E}_{\text{src}}, \mathbf{E}_{\text{trg}}$, confidence of labels of two graphs $w_{\text{src}}, w_{\text{trg}}$

$\mathcal{V}'_{\text{src}}, \mathcal{V}'_{\text{trg}} \leftarrow$ sample subgraphs respectively from $\mathcal{G}_{\text{src}}, \mathcal{G}_{\text{trg}}$ ▷ ST-PPR based Subgraph Sampling 1
$s \leftarrow \min\{|\mathcal{V}'_{\text{src}}|, |\mathcal{V}'_{\text{trg}}|\}$
$\mathcal{V}'_{\text{src}} \leftarrow \mathcal{V}'_{\text{src}}[:s], \mathcal{V}'_{\text{trg}} \leftarrow \mathcal{V}'_{\text{trg}}[:s]$
$\phi \leftarrow$ Make the one-to-one mapping from $\mathcal{V}'_{\text{src}}$ to $\mathcal{V}'_{\text{trg}}$
$\mathcal{E}'_{\text{trg}} \leftarrow \{(u,v)|(u,v) \in \mathcal{E}_{\text{trg}} \wedge \neg(u \in \mathcal{V}'_{\text{trg}} \wedge v \in \mathcal{V}'_{\text{trg}})\}$
$\mathcal{E}'_{\text{src}} \leftarrow \{(\phi(u), \phi(v))|(u,v) \in \mathcal{E}_{\text{src}} \wedge (u \in \mathcal{V}'_{\text{src}} \wedge v \in \mathcal{V}'_{\text{src}})\}$
$\mathcal{V}_{\text{mix}}, \mathcal{E}_{\text{mix}}, \mathbf{X}_{\text{mix}} \leftarrow \mathcal{V}_{\text{trg}}, \mathcal{E}'_{\text{src}} \cup \mathcal{E}'_{\text{trg}}, \mathbf{X}_{\text{trg}}$
$\mathbf{X}_{\text{mix}}[\phi(\mathcal{V}'_{\text{src}})] \leftarrow \mathbf{X}_{\text{src}}[\mathcal{V}'_{\text{src}}]$
$\mathbf{A}_{\text{mix}} \leftarrow$ densify the edge set $\mathcal{E}_{\text{mix}}$
$w_{\text{src}}, w_{\text{trg}} \leftarrow 1 - |\mathcal{E}'_{\text{trg}}|/|\mathcal{E}_{\text{mix}}|, |\mathcal{E}'_{\text{trg}}|/|\mathcal{E}_{\text{mix}}|$
$\mathbf{E}_{\text{src}}, \mathbf{E}_{\text{trg}} \leftarrow$ use one hot vectors to record nodes in $\mathcal{V}_{\text{mix}}$ originated from $\mathcal{V}'_{\text{src}}$ and $\mathcal{V}'_{\text{trg}}$

3.3 Multi-view Decomposition and Learning

From a model perspective, ensembles of diverse neural networks can be seen as learning varied representations of views, thereby improving generalization [4]. However, combining several networks with multiple forward passes leads to high computational costs.

We introduce an innovative pipeline for multi-view decomposition and learning, which activates two sub-networks within a single GNN with minimal computational overhead. During training, we utilize a dual-output predictor with mixed and multi-view loss functions to ensure the learning of multi-view from an optimization perspective.

3.3.1 Mixed-view Encoding

We utilize standard GNNs to encode the mixed-view graph $\mathcal{G}_{\text{mix}}$, which typically leverage repeated message passing process. The process of the l-th message passing $\text{MPNN}_l(\cdot)$ in GNNs is formulated as follows:

$$\mathbf{H}^{(l)}_{\text{mix}} = \text{MPNN}_l\left(\mathbf{H}^{(l-1)}_{\text{mix}}, \mathbf{A}_{\text{mix}}\right), \tag{3}$$

where $\mathbf{H}^{(l)}$ denotes the l-th layer output of our GMV. We consider the node features $\mathbf{X}_{\text{mix}}$ of $\mathcal{G}_{\text{mix}}$ as $\mathbf{H}^{(0)}_{\text{mix}}$ during training. The output of the mixed-view encoder in GNN as $\mathbf{H}^{(L)}_{\text{mix}}$.

Moreover, we also consider GraphGPS [23] as the shared graph transformer backbone. For each layer of GraphGPS, it consists of three components, including $\text{MPNN}_l(\cdot)$, $\text{GlobalAttn}_l(\cdot)$ and $\text{MLP}_l(\cdot)$. Therefore, the process can be decribed as follows:

$$\mathbf{H}^{(l)}_{\text{mix}} \leftarrow \text{MLP}_l(\text{GlobalAttn}_l(\mathbf{H}^{(l)}_{\text{mix}})). \tag{4}$$

3.3.2 Multi-view Decomposition

Diverse views offer greater evidence for GNN to classify graphs. Given mixed-view representation $\mathbf{H}^{(L)}_{\text{mix}}$, we introduce a Multi-View Decomposition (MVD) to obtain three view representations, denoted as $\{\text{View}_i \mid i \in \{\text{src}, \text{trg}, \text{mix}\}\}$. The MVD can be formulated as follows:

$$\mathbf{View}_i = \mathbf{E}_i \mathbf{H}^{(L)}_{\text{mix}}, \tag{5}$$

where $\{\mathbf{E}_i \mid i \in \{\text{src}, \text{trg}, \text{mix}\}\}$ are assignment matrices, which are calculated in Sec 3.2.2. Then, we utilize a common mean pooling layer [21, 46, 47], denoted as $\text{Pool}(\cdot)$, to respectively readout graph representations of diverse views, i.e., $\{\mathbf{p}_i \mid i \in \{\text{src}, \text{trg}, \text{mix}\}\}$:

$$\mathbf{p}_i = \text{Pool}(\mathbf{View}_i). \tag{6}$$

	Method	IMDBB	PROTEINS	NCI1	NCI109	REDDITB	IMDBM	REDDIT-M5	COLLAB
	#graphs	1000	1113	4110	4127	2000	1500	4999	5000
	#classes	2	2	2	2	2	2	3	5
	#avg nodes	19.8	39.1	29.9	29.7	429.6	13.0	508.5	74.5
	#avg edges	96.5	72.8	32.3	32.1	497.8	65.9	594.9	2457.2
GCN	Vanilla	72.30±4.34	72.15±3.75	72.38±2.15	70.27±2.68	87.60±2.55	49.00±3.96	50.83±3.92	81.16±1.72
	DropEdge	72.10±4.21	73.41±4.25	73.94±2.73	67.19±2.42	89.25±3.03	48.87±3.07	50.29±2.21	81.56±0.88
	DropNode	73.30±2.76	72.69±4.25	73.07±2.96	69.76±1.91	88.45±2.64	49.93±3.56	53.73±2.98	81.50±2.32
	Subgraph	72.70±5.16	73.05±3.70	72.60±2.37	69.13±2.72	89.30±2.61	49.27±3.83	50.09±3.45	81.42±1.21
	M-Mixup	73.70±4.12	72.15±4.26	65.16±2.48	62.92±2.15	87.60±3.67	49.80±3.90	48.91±2.08	75.58±1.72
	G-Mixup	73.20±5.60	71.18±3.32	72.75±1.72	72.23±2.50	86.85±2.30	49.33±3.67	51.77±1.42	81.17±1.70
	Submix	73.80±3.57	73.50±5.38	75.40±2.18	72.91±8.25	87.90±3.92	49.00±3.75	53.11±2.03	82.62±2.12
	S-Mixup	72.50±2.20	72.42±4.19	67.27±2.33	69.57±2.56	88.50±1.24	49.93±3.51	51.69±2.21	81.48±1.28
	Ensemble	73.60±4.63	72.60±3.45	73.58±2.25	70.29±2.26	90.45±1.75	49.60±4.26	53.35±2.59	82.52±1.24
	G-MIMO	72.70±2.53	73.41±4.37	76.16±2.47	72.16±3.16	90.15±1.73	50.93±3.45	54.05±4.05	82.36±1.53
	GMV	**75.50±3.67**	**74.67±5.84**	**76.96±2.33**	**76.86±2.15**	**91.40±2.26**	**51.53±2.58**	**54.15±3.15**	**83.92±1.73**
GIN	Vanilla	71.70±3.10	64.70±6.42	78.47±2.41	78.97±1.72	90.10±1.77	48.67±3.75	53.89±2.15	80.48±1.37
	DropEdge	71.70±4.03	68.29±4.01	76.45±2.76	75.33±2.02	89.90±2.17	50.00±4.38	54.19±2.23	79.78±1.65
	DropNode	74.00±4.63	72.51±2.53	78.98±1.86	78.77±1.92	90.55±1.92	51.00±3.00	55.23±2.34	80.16±1.71
	Subgraph	73.20±3.25	72.24±5.76	77.57±2.71	77.32±1.71	88.50±2.97	49.07±3.84	53.37±2.61	80.66±1.75
	M-Mixup	73.10±4.21	71.97±3.75	78.52±2.05	81.03±0.88	82.25±3.87	49.80±3.90	51.49±2.01	80.18±1.31
	G-Mixup	72.40±5.64	64.69±3.60	78.20±1.58	79.75±2.70	90.20±2.84	49.93±2.82	54.33±1.99	80.18±1.62
	Submix	72.50±4.94	69.81±4.57	82.90±2.45	81.04±1.57	90.20±1.95	49.80±4.22	54.59±3.29	82.60±1.73
	S-Mixup	72.80±3.82	67.57±3.50	69.03±1.61	69.57±2.56	87.00±4.25	48.53±3.38	52.75±2.53	79.50±1.25
	Ensemble	74.00±3.10	73.50±3.04	80.34±2.56	80.15±1.83	**92.70±1.87**	49.80±2.91	55.19±2.58	81.58±1.55
	G-MIMO	73.40±2.23	73.70±2.65	80.83±1.83	81.02±2.49	91.50±1.88	50.40±4.78	55.03±3.01	81.24±1.50
	GMV	**74.20±3.37**	**74.40±3.95**	**82.38±2.15**	**82.53±1.95**	92.50±1.30	**52.27±3.67**	**55.35±2.41**	**83.02±1.47**

Table 1: Comparison between GMV and other baselines are conducted on TUDataset benchmark.

3.3.3 Multi-view Learning

During training, we employ a three-layer multilayer perceptron (MLP) as a predictor to simultaneously classify diverse views. Unlike traditional ensemble methods, we simply double the output dimension of the predictor, transforming it into a dual-output predictor that generates two outputs. It can guide the shared backbone to facilitate the cost-effective realization of two sub-networks:

$$\hat{\mathbf{y}}_i^1, \hat{\mathbf{y}}_i^2 = \text{Predictor}(\mathbf{p}_i), \tag{7}$$

where $i \in \{\text{src}, \text{trg}, \text{mix}\}$. Moreover, to optimize GNN with these diverse views, we propose the mixed-view loss ℓ_{mix} and the multi-view loss ℓ_{view}:

$$\ell_{\text{mix}} = w_{\text{src}}\text{CE}(\hat{\mathbf{y}}_{\text{mix}}^1, \mathbf{y}_{\text{src}}) + w_{\text{trg}}\text{CE}(\hat{\mathbf{y}}_{\text{mix}}^2, \mathbf{y}_{\text{trg}}), \tag{8}$$

$$\ell_{\text{view}} = \text{CE}(\hat{\mathbf{y}}_{\text{src}}^1, \mathbf{y}_{\text{src}}) + \text{CE}(\hat{\mathbf{y}}_{\text{trg}}^2, \mathbf{y}_{\text{trg}}), \tag{9}$$

w_{src} and w_{trg} are considered as confidence of labels of two graphs, calculated in Equation (2). The mixed-view loss ℓ_{mix} helps GNN inferring partial labels of $\mathcal{G}_{\text{src}}$ and $\mathcal{G}_{\text{trg}}$, playing a role of regularization, while the multi-view loss ℓ_{view} directly boosts the capacity of diverse view representations of GNN. These two losses collectively improve the diversity of sub-networks integrated into GNN, enhancing the generalization and robustness:

$$\ell = \ell_{\text{mix}} + \alpha\ell_{\text{view}} + R(\theta), \tag{10}$$

where ℓ is the final loss, α is the hyper parameter and $R(\theta)$ denotes the regularization item, e.g., l_2 norm. The detail of multi-view learning process is in the Algorithm 3 of Appendix 6.2.

3.4 Inference

During inference, GMV processes unseen input $\mathcal{G}_{\text{test}}$ via a standard forward pass. The primary distinction of GMV from standard GNNs lies in its dual prediction heads. Unlike the training phase, subgraph processing and multi-view decomposition are not required during inference. The final prediction is obtained by averaging the outputs of the dual prediction heads. This approach effectively acts as an efficient ensemble within a single model, leveraging the benefits of multi-view learning:

$$f_\theta\left(\hat{\mathbf{y}}_{\text{test}} \mid \mathcal{G}_{\text{test}}\right) = \frac{1}{2}\sum_{m=1}^{2} f_\theta\left(\hat{\mathbf{y}}^{(m)} \mid \mathcal{G}_{\text{test}}\right). \tag{11}$$

4 Experiments

Baselines.

GCN [19], GIN [21] are utilized as GNN backbones, and GraphGPS [23] is selected as the GT backbone. We evaluate our effectiveness of GMV compared with graph augmentation methods, such as DropEdge [6], DropNode [30] Subgraph [31], M-Mixup [48] , G-Mixup [49] and SubMix [33].

For ensemble learning [9], we consider an classic ensemble and G-MIMO [37]. For fair comparison, we only consider ensemble of two networks/sub-networks.

	Method	HIV	BBBP	BACE	PPA
	#graphs	41127	2039	1513	158100
	#classes	3	2	2	2
	#avg nodes	25.5	24.1	34.1	243.4
	#avg edges	54.9	26.0	36.9	2266.1
GCN	Vanilla	75.38±0.21	65.74±0.17	77.74±0.23	68.33 ±0.33
	Submix	75.63±0.17	65.90±0.54	78.00±0.32	68.97 ±0.39
	G-MIMO	75.97±0.18	65.87±0.40	78.23±0.35	70.02 ±0.32
	GMV	**76.16±0.15**	**66.18±0.10**	**78.51±0.32**	**70.21 ±0.21**
GIN	Vanilla	76.01±0.11	66.34±0.32	78.42±0.42	69.00 ±0.18
	Submix	77.00±0.46	67.67±0.29	78.93±0.43	70.43 ±0.23
	G-MIMO	77.43±0.23	68.38±0.43	78.89±0.13	70.08 ±0.18
	GMV	**78.23±0.43**	**68.56±0.31**	**79.43±0.28**	**71.56 ±0.17**
GraphGPS	Vanilla	77.53±0.80	67.84±1.65	80.54±0.87	80.15±0.12
	Submix	78.47±0.94	68.38±1.21	81.21±0.25	80.60±0.33
	G-MIMO	78.65±1.04	68.78±0.86	82.07±2.59	80.88±0.21
	GMV	**80.23±1.02**	**70.32±0.94**	**83.99±0.17**	**81.21±0.32**

Table 2: Comparison between GMV and other baselines are conducted on four OGB benchmark datasets.

Experiment Details. For each method, we conduct 10-fold cross-validation experiments on each dataset from TUDataset Benchmark, calculating the mean accuracy and standard deviation to derive results. Following S-Mixup [7], the datasets are split into training, validation and test sets. Specifically, 80% for training, 10% for validation, and 10% for testing. For the datasets from OGB Graph Banchmark [50], we adopt the public train/validation/test splits, and report the results of the test set. We conduct each experiment three times and utilize area under curve (AUC) as measurement on these OGB graph datasets. All experiments are conducted on NVIDIA 3090TI GPUs.

Datasets. We consider different sizes and numbers of graphs to evaluate the performance of our proposed method. Table 1 and Table 2 outlines the specifics of eight real-world datasets from the TUDatasets benchmark [51] and three datasets from open graph benchmark (OGB) [52].

4.1 Overall Comparison

Table 1 and Table 2 presents the results of GNNs with GMV alongside other baselines across eight benchmark datasets from TUDataset and four benchmark datasets from OGB. By simultaneously incorporating multi-view learning from the perspectives of model, data, and optimization, GMV significantly improves the average accuracy of both GCN and GIN on the TUDataset benchmark datasets. Unlike other graph augmentation and ensemble methods, which typically expand the "view" from a single perspective, GMV offers a unified and efficient approach.

To evaluate the effectiveness of GMV on large-scale graph classification tasks, we use the widely adopted GraphGPS [23] as the backbone for experiments on OGB datasets and TUDataset. As shown in Table 6a and Table 2, GMV achieves the best performance across all tested datasets. This approach has established state-of-the-art results, further highlighting GMV's superiority over traditional methods. In Appendix 6.3, Table 6, we also conduct experiments on state-of-arts GNNs.

4.2 Generalization and Robustness

Limited Labels for GMV. Following NoisyGL [53], we conduct the comparison study on limited and noisy labeled graph data to demonstrate robustness and generalization of GMV. We adopt 75%, 50%, 25% and 10% training label ratios to verify the generalization of GMV. As shown in Fig 3(a), GMV consistently outperforms other methods with different label ratios, thereby achieving great generalization.

Noisy Labels for GMV. To simulate label noise, we randomly corrupt 10%, 20% and 40% training labels on IMDBB and PROTEINS datasets, while keeping validation and testing datasets unchanged.

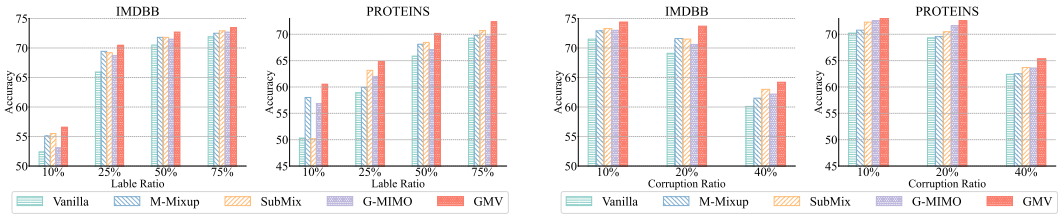

(a) Limited Label Study

(b) Noisy Label Study

Figure 3: Comparison study between GMV and other methods for different ratio of label/varying levels of label corruption on IMDBB and PROTEINS for GCN.

	Vanilla	Random	PPR	BFS	DPP	DPP w. BFS	ST-PPR
IMDBB	72.30±2.84	72.70±5.16	72.60±2.37	73.00±4.36	72.60±3.69	73.20±4.26	**74.10±3.01**
PROTEINS	72.15±3.75	72.60±2.37	73.05±3.70	72.73±1.90	72.84±1.77	72.63±2.61	**74.27±1.61**

Table 3: Comparisons among different subgraph sampling methods for GCN.

As shown in Figure 3(b), GMV achieves better results under different noisy condition, which evaluate the robustness of it.

4.3 Ablation Study

Comparison of View Generation Methods. We first compare the effectiveness of our proposed ST-PPR with other subgraph sampling methods. Vanilla indicates the GCN without graph augmentations. As shown in Table 3, our subgraph sampling method achieves the best performance among them because it considers both structure and semantic information. Moreover, we investigate the effectiveness of ST-PPR, SubMix and ST-SubMix. As depicted in Table 4(a), ST-SubMix achieves higher accuracy than SubMix by considering the property of the structure. In Appendix 6.4, Table 7b, we also compare different graph augmentation methods for G-MIMO to generate richer training samples. These methods yield lower accuracy than GMV, thereby verifying the effectiveness of GMV.

Ablation of MVG and MVD. We examine the efficacy of mixed-view generation (MVG) and multi-view decomposition (MVD) for GMV (GCN) on the IMDBB and PROTEINS datasets. The results, reported in Table 4(b), show that both MVG and MVD play a crucial role in enhancing performance. Combining these two achieves the best performance, which implies that expanding views from both data and model perspectives simultaneously can help the model learn better multi-view representations. More details can be found in the When only "MVG" is applied, GMV enhances GNN performance from a data perspective, playing a same role of ST-SubMix. In contrast, with only "MVD" GMV boosts GNNs from a model perspective. With consistent graph pair inputs, GMV modifies the GNN structure in a manner the same as G-MIMO [37]. Unlike simply increasing the size of the prediction head [54], this approach leverages distinct graphs to activate different sub-networks within the GNN, achieving a simple ensemble. These two methods respectively improve of GCN, as shown in Table 4b.

Ablation of Mixed-view/Multi-view Loss. Additionally, we conduct an ablation study to verify the impact of mixed-view loss and multi-view loss in the GMV framework on the IMDBB dataset. As shown in Table 4(c), these two losses collectively enhance the accuracy of the GNN. When we only adopt each of these losses, GMV achieves lower accuracy than when both are considered. Therefore, both losses are necessary to encourage sub-networks to learn from mixed and multi-views, thereby enhancing the multi-view learning ability from an optimization perspective.

4.4 Efficiency Study

During inference, GMV requires only a single forward pass of standard GNNs with an additional prediction head. Consequently, GMV's time complexity is nearly identical to that of standard GNNs, as illustrated in Fig 1, where GMV demonstrates the optimal balance between accuracy and computational overhead. As for training, the mixed-view generation process can be preprocessed only once to obtain sampled nodes for each graph, therefore significantly accelerating the training

Methods	IMDBB	PROTEINS
Vanilla	72.30±4.34	72.15±3.75
SubMix	73.80±3.57	73.50±5.38
ST-PPR	**74.10±3.01**	72.87±4.09
ST-SubMix	**74.10±3.66**	**74.40±5.98**

(a) Comparison of VG

/w. MVG	/w. MVD	IMDBB	PROTEINS
		72.30±4.34	72.15±3.75
✓		74.10±3.66	74.40±5.98
	✓	72.70±2.53	73.41±4.37
✓	✓	**75.50±3.67**	**74.67±5.84**

(b) Ablation of Components

/w. ℓ_{mix}	/w. ℓ_{view}	IMDBB	PROTEINS
		72.30±4.34	72.15±3.75
✓		74.55±2.32	74.60±2.38
	✓	74.55±3.18	73.87±3.95
✓	✓	**75.50±3.67**	**74.67±5.84**

(c) Ablation of Losses

Table 4: Results of ablation studies. (a) Comparison of different view generation methods (VG) including our proposed ST-PPR and ST-SubMix. (b) Ablation of two components of our proposed GMV. (c) Ablation of our proposed mixed-view loss (ℓ_{mix}) and multi-view loss (ℓ_{view}).

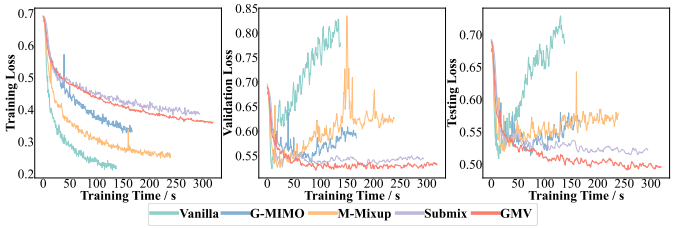

Figure 4: Training Time v.s. Training/Validation/Testing Loss on IMDBB.

	D_{Disagree}	D_{KL}	Accuracy
Vanilla	0	0	70.27
Submix	0	0	72.91
Ensemble	10.02	1.56	70.29
G-MIMO	12.14	1.63	72.16
GMV	13.40	5.41	**76.86**

Table 5: Comparison of prediction on NCI109 between dual sub-networks of GMV and baselines within GCN.

process. Specifically, given $\mathcal{G}_{\text{src}}$ and $\mathcal{G}_{\text{trg}}$, the time complexity of mixed-view generation process is $O(|\mathcal{V}_{\text{src}}| + |\mathcal{V}_{\text{trg}}|)$. We monitor the evolution of training and validation loss over time in Fig 4. While the vanilla GCN converges fastest, it suffers from significant overfitting. In contrast, graph augmentation techniques like M-Mixup and Submix, along with the ensemble method G-MIMO, help mitigate overfitting to some extent. our GMV framework inherently functions as a more powerful regularizer compared to these standard methods. This is evidenced by GMV achieving a lower validation loss and, consequently, better generalization to the test set.

4.5 Quantitative Study of Diversity.

We evaluate the diversity of predictions made by GCN within GMV and other baseline methods on the NCI109 dataset. We employ disagreement [11](D_{Disagree}) and average Kullback-Leibler divergence [13] (D_{KL}) as diversity metrics. Suppose f_1 and f_2 are two (sub-)networks. D_{Disagree} is computed as $\sum_{\mathcal{G}\in\mathbb{G}} \mathbb{1}(f_1(\mathcal{G}) \neq f_2(\mathcal{G}))$, where $\mathbb{1}(\cdot)$ equals 1 only if $f_1(\mathcal{G}) \neq f_2(\mathcal{G})$. D_{KL}, is calculated as $\frac{1}{2}(\text{KL}(\hat{y}_1||\hat{y}_2) + \text{KL}(\hat{y}_2||\hat{y}_1)) = \frac{1}{2}(\mathbb{E}_{\hat{y}_2}(\log \hat{y}_2 - \log \hat{y}_1) + \mathbb{E}_{\hat{y}_1} \log(\hat{y}_1 - \log \hat{y}_2)$. As shown in Table 5, GMV achieves higher D_{Disagree}, D_{KL} and accuracy, indicating an enhanced capacity to represent diverse views for better generalization.

5 Conclusion

We have introduced GMV, an unified and efficient framework that significantly enhances the robustness and generalization capabilities of GNNs/GTs in graph classification. During training, GMV encourages GNNs/GTs to explore diverse views by integrating data, model, and optimization perspectives through a mixed view generation and multi-view decomposition and learning pipeline. During inference, GMV appends an additional prediction head to standard GNNs/GTs, enabling superior performance in a single forward pass with ensemble-like behavior. Our extensive experiments across various datasets demonstrate that GMV consistently outperforms existing augmentation and ensemble techniques, establishing it as a highly effective and promising method to improve the performance and generalization of GNNs/GTs.

Acknowledgments and Disclosure of Funding

This work is supported by National Natural Science Foundation of China (NSFC 62176059, 62576103). The computations in this research were performed using the CFFF platform of Fudan University.

References

[1] Wanyu Lin, Zhaolin Gao, and Baochun Li. Shoestring: Graph-based semi-supervised classification with severely limited labeled data. In *CVPR*, 2020.

[2] Jie Chen, Shouzhen Chen, Mingyuan Bai, Jian Pu, Junping Zhang, and Junbin Gao. Graph decoupling attention markov networks for semisupervised graph node classification. *TNNLS*, 2022.

[3] Guohao Li, Matthias Müller, Bernard Ghanem, and Vladlen Koltun. Training graph neural networks with 1000 layers. In *ICML*, 2021.

[4] Umar Asif, Jianbin Tang, and Stefan Harrer. Towards understanding ensemble, knowledge distillation and self-distillation in deep learning. In *ICLR*, 2023.

[5] Andrew Saxe, Stephanie Nelli, and Christopher Summerfield. If deep learning is the answer, what is the question? *Nature Reviews Neuroscience*, 2021.

[6] Yu Rong, Wenbing Huang, Tingyang Xu, and Junzhou Huang. Dropedge: Towards deep graph convolutional networks on node classification. In *ICLR*, 2020.

[7] Hongyi Ling, Zhimeng Jiang, Meng Liu, Shuiwang Ji, and Na Zou. Graph mixup with soft alignments. In *ICML*, 2023.

[8] Kaize Ding, Zhe Xu, Hanghang Tong, and Huan Liu. Data augmentation for deep graph learning: A survey. *SIGKDD*, 2022.

[9] Lars Kai Hansen and Peter Salamon. Neural network ensembles. *TPAMI*, 1990.

[10] Yeming Wen, Dustin Tran, and Jimmy Ba. Batchensemble: an alternative approach to efficient ensemble and lifelong learning. In *ICLR*, 2020.

[11] Stanislav Fort, Huiyi Hu, and Balaji Lakshminarayanan. Deep ensembles: A loss landscape perspective. In *ICLR*, 2020.

[12] Jonathan Frankle and Michael Carbin. lottery ticket hypothesis: Finding sparse, trainable neural networks. In *ICLR*, 2019.

[13] Marton Havasi, Rodolphe Jenatton, Stanislav Fort, Jeremiah Zhe Liu, Jasper Snoek, Balaji Lakshminarayanan, Andrew M Dai, and Dustin Tran. Training independent subnetworks for robust prediction. In *ICLR 2021*, 2021.

[14] Justin Gilmer, Samuel S Schoenholz, Patrick F Riley, Oriol Vinyals, and George E Dahl. Neural message passing for quantum chemistry. In *ICML*, 2017.

[15] Jie Chen, Weiqi Liu, and Jian Pu. Memory-based message passing: Decoupling the message for propagation from discrimination. In *ICASSP*, 2022.

[16] Zonghan Wu, Shirui Pan, Fengwen Chen, Guodong Long, Chengqi Zhang, and Philip S Yu. A comprehensive survey on graph neural networks. *TNNLS*, 2020.

[17] Jie Chen, Zilong Li, Yin Zhu, Junping Zhang, and Jian Pu. From node interaction to hop interaction: New effective and scalable graph learning paradigm. In *CVPR*, 2023.

[18] Jie Chen, Shouzhen Chen, Junbin Gao, Zengfeng Huang, Junping Zhang, and Jian Pu. Exploiting neighbor effect: Conv-agnostic gnn framework for graphs with heterophily. *TNNLS*, 2023.

[19] Thomas N. Kipf and Max Welling. Semi-supervised classification with graph convolutional networks. In *ICLR*, 2017.

[20] Hamilton Will, Ying Zhitao, and Leskovec Jure. Inductive representation learning on large graphs. In *NeurIPS*, 2020.

[21] Keyulu Xu, Weihua Hu, Jure Leskovec, and Stefanie Jegelka. How powerful are graph neural networks? In *ICLR*, 2019.

[22] Chengxuan Ying, Tianle Cai, Shengjie Luo, Shuxin Zheng, Guolin Ke, Di He, Yanming Shen, and Tie-Yan Liu. Do transformers really perform badly for graph representation? *NeurIPS*, 2021.

[23] Ladislav Rampášek, Michael Galkin, Vijay Prakash Dwivedi, Anh Tuan Luu, Guy Wolf, and Dominique Beaini. Recipe for a general, powerful, scalable graph transformer. *NeurIPS*, 2022.

[24] Xiaoqiang Yan, Shizhe Hu, Yiqiao Mao, Yangdong Ye, and Hui Yu. Deep multi-view learning methods: A review. *Neurocomputing*, 2021.

[25] Xiao Luo, Yusheng Zhao, Zhengyang Mao, Yifang Qin, Wei Ju, Ming Zhang, and Yizhou Sun. Rignn: A rationale perspective for semi-supervised open-world graph classification. *TMLR*, 2023.

[26] Jia Wu, Zhibin Hong, Shirui Pan, Xingquan Zhu, Zhihua Cai, and Chengqi Zhang. Multi-graph-view subgraph mining for graph classification. *Knowledge and Information Systems*, 2016.

[27] Jinliang Yuan, Hualei Yu, Meng Cao, Ming Xu, Junyuan Xie, and Chongjun Wang. Semi-supervised and self-supervised classification with multi-view graph neural networks. In *CIKM*, 2021.

[28] Bo Liu, Zhiyong Che, Haowen Zhong, and Yanshan Xiao. A ranking based multi-view method for positive and unlabeled graph classification. *TKDE*, 2021.

[29] Qipeng Zhu, Xiong Wang, Zhihong Lu, Jiangwei Lao, Congyun Jin, Jie Chen, Yingzhe Peng, Qi Zhu, Lianzhen Zhong, Jiajia Liu, et al. Admire: Adaptive method to enhance multiple image resolutions in text-rich multi-image understanding. In *SIGKDD*, pages 5237–5248, 2025.

[30] Wenzheng Feng, Jie Zhang, Yuxiao Dong, Yu Han, Huanbo Luan, Qian Xu, Qiang Yang, Evgeny Kharlamov, and Jie Tang. Graph random neural networks for semi-supervised learning on graphs. In *NeurIPS*, 2020.

[31] Yuning You, Tianlong Chen, Yongduo Sui, Ting Chen, Zhangyang Wang, and Yang Shen. Graph contrastive learning with augmentations. In *NeurIPS*, 2020.

[32] Hongyi Zhang, Moustapha Cissé, Yann N. Dauphin, and David Lopez-Paz. Mixup: Beyond empirical risk minimization. In *ICLR*, 2018.

[33] Jaemin Yoo, Sooyeon Shim, and U Kang. Model-agnostic augmentation for accurate graph classification. In *WWW*, 2022.

[34] Joonhyung Park, Hajin Shim, and Eunho Yang. Graph transplant: Node saliency-guided graph mixup with local structure preservation. In *AAAI*, 2022.

[35] Yingzhe Peng, Gongrui Zhang, Miaosen Zhang, Zhiyuan You, Jie Liu, Qipeng Zhu, Kai Yang, Xingzhong Xu, Xin Geng, and Xu Yang. Lmm-r1: Empowering 3b lmms with strong reasoning abilities through two-stage rule-based rl. *arXiv preprint arXiv:2503.07536*, 2025.

[36] Tianlong Chen, Yongduo Sui, Xuxi Chen, Aston Zhang, and Zhangyang Wang. A unified lottery ticket hypothesis for graph neural networks. In *ICML*, 2021.

[37] Qipeng Zhu, Jie Chen, Junping Zhang, and Jian Pu. G-mimo: Empowering gnns with diverse sub-networks for graph classification. In *ICME*, 2024.

[38] Ryan A Rossi, Nesreen K Ahmed, Eunyee Koh, Sungchul Kim, Anup Rao, and Yasin Abbasi-Yadkori. A structural graph representation learning framework. In *WSDM*, pages 483–491, 2020.

[39] Xin Liu, Mingyu Yan, Lei Deng, Guoqi Li, Xiaochun Ye, and Dongrui Fan. Sampling methods for efficient training of graph convolutional networks: A survey. *IEEE/CAA Journal of Automatica Sinica*, 2021.

[40] Christian Hübler, Hans-Peter Kriegel, Karsten Borgwardt, and Zoubin Ghahramani. Metropolis algorithms for representative subgraph sampling. In *ICDM*, 2008.

[41] Johannes Klicpera, Stefan Weißenberger, and Stephan Günnemann. Diffusion improves graph learning. In *NeurIPS*, 2019.

[42] Wei Duan, Junyu Xuan, Maoying Qiao, and Jie Lu. Learning from the dark: boosting graph convolutional neural networks with diverse negative samples. In *AAAI*, 2022.

[43] Wei Duan, Jie Lu, Yu Guang Wang, and Junyu Xuan. Layer-diverse negative sampling for graph neural networks. *arXiv preprint arXiv:2403.11408*, 2024.

[44] Hanqing Zeng, Muhan Zhang, Yinglong Xia, Ajitesh Srivastava, Andrey Malevich, Rajgopal Kannan, Viktor Prasanna, Long Jin, and Ren Chen. Decoupling the depth and scope of graph neural networks. *NeurIPS*, 2021.

[45] Dexter C Kozen and Dexter C Kozen. Depth-first and breadth-first search. *The design and analysis of algorithms*, 1992.

[46] Zhitao Ying, Jiaxuan You, Christopher Morris, Xiang Ren, William L. Hamilton, and Jure Leskovec. Hierarchical graph representation learning with differentiable pooling. In *NeurIPS*, 2018.

[47] Yao Ma, Suhang Wang, Charu C. Aggarwal, and Jiliang Tang. Graph convolutional networks with eigenpooling. In *SIGKDD*, 2019.

[48] Vikas Verma, Alex Lamb, Christopher Beckham, Amir Najafi, Ioannis Mitliagkas, David Lopez-Paz, and Yoshua Bengio. Manifold mixup: Better representations by interpolating hidden states. In *ICML*, 2019.

[49] Xiaotian Han, Zhimeng Jiang, Ninghao Liu, and Xia Hu. G-mixup: Graph data augmentation for graph classification. In *ICML*, 2022.

[50] Weihua Hu, Matthias Fey, Marinka Zitnik, Yuxiao Dong, Hongyu Ren, Bowen Liu, Michele Catasta, and Jure Leskovec. Open graph benchmark: Datasets for machine learning on graphs. *NeurIPS*, 2020.

[51] Christopher Morris, Nils M. Kriege, Franka Bause, Kristian Kersting, Petra Mutzel, and Marion Neumann. Tudataset: A collection of benchmark datasets for learning with graphs. *CoRR*, 2020.

[52] Weihua Hu, Matthias Fey, Marinka Zitnik, Yuxiao Dong, Hongyu Ren, Bowen Liu, Michele Catasta, and Jure Leskovec. Open graph benchmark: Datasets for machine learning on graphs. *NeurIPS*, 2020.

[53] Zhonghao Wang, Danyu Sun, Sheng Zhou, Haobo Wang, Jiapei Fan, Longtao Huang, and Jiajun Bu. Noisygl: A comprehensive benchmark for graph neural networks under label noise. *arXiv preprint arXiv:2406.04299*, 2024.

[54] Stefan Lee, Senthil Purushwalkam, Michael Cogswell, David Crandall, and Dhruv Batra. Why m heads are better than one: Training a diverse ensemble of deep networks. *arXiv e-prints*, 2015.

[55] David Buterez, Jon Paul Janet, Dino Oglic, and Pietro Liò. An end-to-end attention-based approach for learning on graphs. *Nature Communications*, 16(1):5244, 2025.

NeurIPS Paper Checklist

1. **Claims**

   Question: Do the main claims made in the abstract and introduction accurately reflect the paper's contributions and scope?

   Answer: [Yes]

   Guidelines:

   - The answer NA means that the abstract and introduction do not include the claims made in the paper.
   - The abstract and/or introduction should clearly state the claims made, including the contributions made in the paper and important assumptions and limitations. A No or NA answer to this question will not be perceived well by the reviewers.
   - The claims made should match theoretical and experimental results, and reflect how much the results can be expected to generalize to other settings.
   - It is fine to include aspirational goals as motivation as long as it is clear that these goals are not attained by the paper.

2. **Limitations**

   Question: Does the paper discuss the limitations of the work performed by the authors?

   Answer: [Yes] See limitations in Appendix 6.8.

   Guidelines:

   - The answer NA means that the paper has no limitation while the answer No means that the paper has limitations, but those are not discussed in the paper.
   - The authors are encouraged to create a separate "Limitations" section in their paper.
   - The paper should point out any strong assumptions and how robust the results are to violations of these assumptions (e.g., independence assumptions, noiseless settings, model well-specification, asymptotic approximations only holding locally). The authors should reflect on how these assumptions might be violated in practice and what the implications would be.
   - The authors should reflect on the scope of the claims made, e.g., if the approach was only tested on a few datasets or with a few runs. In general, empirical results often depend on implicit assumptions, which should be articulated.
   - The authors should reflect on the factors that influence the performance of the approach. For example, a facial recognition algorithm may perform poorly when image resolution is low or images are taken in low lighting. Or a speech-to-text system might not be used reliably to provide closed captions for online lectures because it fails to handle technical jargon.
   - The authors should discuss the computational efficiency of the proposed algorithms and how they scale with dataset size.
   - If applicable, the authors should discuss possible limitations of their approach to address problems of privacy and fairness.
   - While the authors might fear that complete honesty about limitations might be used by reviewers as grounds for rejection, a worse outcome might be that reviewers discover limitations that aren't acknowledged in the paper. The authors should use their best judgment and recognize that individual actions in favor of transparency play an important role in developing norms that preserve the integrity of the community. Reviewers will be specifically instructed to not penalize honesty concerning limitations.

3. **Theory Assumptions and Proofs**

   Question: For each theoretical result, does the paper provide the full set of assumptions and a complete (and correct) proof?

   Answer: [Yes] See in Appendix 6.1.

   Guidelines:

   - The answer NA means that the paper does not include theoretical results.

- All the theorems, formulas, and proofs in the paper should be numbered and cross-referenced.
- All assumptions should be clearly stated or referenced in the statement of any theorems.
- The proofs can either appear in the main paper or the supplemental material, but if they appear in the supplemental material, the authors are encouraged to provide a short proof sketch to provide intuition.
- Inversely, any informal proof provided in the core of the paper should be complemented by formal proofs provided in appendix or supplemental material.
- Theorems and Lemmas that the proof relies upon should be properly referenced.

4. **Experimental Result Reproducibility**

   Question: Does the paper fully disclose all the information needed to reproduce the main experimental results of the paper to the extent that it affects the main claims and/or conclusions of the paper (regardless of whether the code and data are provided or not)?

   Answer: [Yes] See in Sec 4

   Guidelines:

   - The answer NA means that the paper does not include experiments.
   - If the paper includes experiments, a No answer to this question will not be perceived well by the reviewers: Making the paper reproducible is important, regardless of whether the code and data are provided or not.
   - If the contribution is a dataset and/or model, the authors should describe the steps taken to make their results reproducible or verifiable.
   - Depending on the contribution, reproducibility can be accomplished in various ways. For example, if the contribution is a novel architecture, describing the architecture fully might suffice, or if the contribution is a specific model and empirical evaluation, it may be necessary to either make it possible for others to replicate the model with the same dataset, or provide access to the model. In general. releasing code and data is often one good way to accomplish this, but reproducibility can also be provided via detailed instructions for how to replicate the results, access to a hosted model (e.g., in the case of a large language model), releasing of a model checkpoint, or other means that are appropriate to the research performed.
   - While NeurIPS does not require releasing code, the conference does require all submissions to provide some reasonable avenue for reproducibility, which may depend on the nature of the contribution. For example
     (a) If the contribution is primarily a new algorithm, the paper should make it clear how to reproduce that algorithm.
     (b) If the contribution is primarily a new model architecture, the paper should describe the architecture clearly and fully.
     (c) If the contribution is a new model (e.g., a large language model), then there should either be a way to access this model for reproducing the results or a way to reproduce the model (e.g., with an open-source dataset or instructions for how to construct the dataset).
     (d) We recognize that reproducibility may be tricky in some cases, in which case authors are welcome to describe the particular way they provide for reproducibility. In the case of closed-source models, it may be that access to the model is limited in some way (e.g., to registered users), but it should be possible for other researchers to have some path to reproducing or verifying the results.

5. **Open access to data and code**

   Question: Does the paper provide open access to the data and code, with sufficient instructions to faithfully reproduce the main experimental results, as described in supplemental material?

   Answer: [Yes] We provide the pseudocode in Sec 3 and Appendix 6.2.

   Guidelines:

   - The answer NA means that paper does not include experiments requiring code.

- Please see the NeurIPS code and data submission guidelines (`https://nips.cc/public/guides/CodeSubmissionPolicy`) for more details.
- While we encourage the release of code and data, we understand that this might not be possible, so "No" is an acceptable answer. Papers cannot be rejected simply for not including code, unless this is central to the contribution (e.g., for a new open-source benchmark).
- The instructions should contain the exact command and environment needed to run to reproduce the results. See the NeurIPS code and data submission guidelines (`https://nips.cc/public/guides/CodeSubmissionPolicy`) for more details.
- The authors should provide instructions on data access and preparation, including how to access the raw data, preprocessed data, intermediate data, and generated data, etc.
- The authors should provide scripts to reproduce all experimental results for the new proposed method and baselines. If only a subset of experiments are reproducible, they should state which ones are omitted from the script and why.
- At submission time, to preserve anonymity, the authors should release anonymized versions (if applicable).
- Providing as much information as possible in supplemental material (appended to the paper) is recommended, but including URLs to data and code is permitted.

6. **Experimental Setting/Details**

   Question: Does the paper specify all the training and test details (e.g., data splits, hyperparameters, how they were chosen, type of optimizer, etc.) necessary to understand the results?

   Answer: [Yes]

   Guidelines:

   - The answer NA means that the paper does not include experiments.
   - The experimental setting should be presented in the core of the paper to a level of detail that is necessary to appreciate the results and make sense of them.
   - The full details can be provided either with the code, in appendix, or as supplemental material.

7. **Experiment Statistical Significance**

   Question: Does the paper report error bars suitably and correctly defined or other appropriate information about the statistical significance of the experiments?

   Answer: [Yes] See in Sec 4.

   Guidelines:

   - The answer NA means that the paper does not include experiments.
   - The authors should answer "Yes" if the results are accompanied by error bars, confidence intervals, or statistical significance tests, at least for the experiments that support the main claims of the paper.
   - The factors of variability that the error bars are capturing should be clearly stated (for example, train/test split, initialization, random drawing of some parameter, or overall run with given experimental conditions).
   - The method for calculating the error bars should be explained (closed form formula, call to a library function, bootstrap, etc.)
   - The assumptions made should be given (e.g., Normally distributed errors).
   - It should be clear whether the error bar is the standard deviation or the standard error of the mean.
   - It is OK to report 1-sigma error bars, but one should state it. The authors should preferably report a 2-sigma error bar than state that they have a 96% CI, if the hypothesis of Normality of errors is not verified.
   - For asymmetric distributions, the authors should be careful not to show in tables or figures symmetric error bars that would yield results that are out of range (e.g. negative error rates).

- If error bars are reported in tables or plots, The authors should explain in the text how they were calculated and reference the corresponding figures or tables in the text.

8. **Experiments Compute Resources**

   Question: For each experiment, does the paper provide sufficient information on the computer resources (type of compute workers, memory, time of execution) needed to reproduce the experiments?

   Answer: [Yes] See in Sec 4.

   Guidelines:

   - The answer NA means that the paper does not include experiments.
   - The paper should indicate the type of compute workers CPU or GPU, internal cluster, or cloud provider, including relevant memory and storage.
   - The paper should provide the amount of compute required for each of the individual experimental runs as well as estimate the total compute.
   - The paper should disclose whether the full research project required more compute than the experiments reported in the paper (e.g., preliminary or failed experiments that didn't make it into the paper).

9. **Code Of Ethics**

   Question: Does the research conducted in the paper conform, in every respect, with the NeurIPS Code of Ethics `https://neurips.cc/public/EthicsGuidelines`?

   Answer: [Yes]

   Guidelines:

   - The answer NA means that the authors have not reviewed the NeurIPS Code of Ethics.
   - If the authors answer No, they should explain the special circumstances that require a deviation from the Code of Ethics.
   - The authors should make sure to preserve anonymity (e.g., if there is a special consideration due to laws or regulations in their jurisdiction).

10. **Broader Impacts**

    Question: Does the paper discuss both potential positive societal impacts and negative societal impacts of the work performed?

    Answer: [No]

    Guidelines:

    - The answer NA means that there is no societal impact of the work performed.
    - If the authors answer NA or No, they should explain why their work has no societal impact or why the paper does not address societal impact.
    - Examples of negative societal impacts include potential malicious or unintended uses (e.g., disinformation, generating fake profiles, surveillance), fairness considerations (e.g., deployment of technologies that could make decisions that unfairly impact specific groups), privacy considerations, and security considerations.
    - The conference expects that many papers will be foundational research and not tied to particular applications, let alone deployments. However, if there is a direct path to any negative applications, the authors should point it out. For example, it is legitimate to point out that an improvement in the quality of generative models could be used to generate deepfakes for disinformation. On the other hand, it is not needed to point out that a generic algorithm for optimizing neural networks could enable people to train models that generate Deepfakes faster.
    - The authors should consider possible harms that could arise when the technology is being used as intended and functioning correctly, harms that could arise when the technology is being used as intended but gives incorrect results, and harms following from (intentional or unintentional) misuse of the technology.
    - If there are negative societal impacts, the authors could also discuss possible mitigation strategies (e.g., gated release of models, providing defenses in addition to attacks, mechanisms for monitoring misuse, mechanisms to monitor how a system learns from feedback over time, improving the efficiency and accessibility of ML).

11. **Safeguards**

    Question: Does the paper describe safeguards that have been put in place for responsible release of data or models that have a high risk for misuse (e.g., pretrained language models, image generators, or scraped datasets)?

    Answer: [No]

    Guidelines:

    - The answer NA means that the paper poses no such risks.
    - Released models that have a high risk for misuse or dual-use should be released with necessary safeguards to allow for controlled use of the model, for example by requiring that users adhere to usage guidelines or restrictions to access the model or implementing safety filters.
    - Datasets that have been scraped from the Internet could pose safety risks. The authors should describe how they avoided releasing unsafe images.
    - We recognize that providing effective safeguards is challenging, and many papers do not require this, but we encourage authors to take this into account and make a best faith effort.

12. **Licenses for existing assets**

    Question: Are the creators or original owners of assets (e.g., code, data, models), used in the paper, properly credited and are the license and terms of use explicitly mentioned and properly respected?

    Answer: [Yes]

    Guidelines:

    - The answer NA means that the paper does not use existing assets.
    - The authors should cite the original paper that produced the code package or dataset.
    - The authors should state which version of the asset is used and, if possible, include a URL.
    - The name of the license (e.g., CC-BY 4.0) should be included for each asset.
    - For scraped data from a particular source (e.g., website), the copyright and terms of service of that source should be provided.
    - If assets are released, the license, copyright information, and terms of use in the package should be provided. For popular datasets, `paperswithcode.com/datasets` has curated licenses for some datasets. Their licensing guide can help determine the license of a dataset.
    - For existing datasets that are re-packaged, both the original license and the license of the derived asset (if it has changed) should be provided.
    - If this information is not available online, the authors are encouraged to reach out to the asset's creators.

13. **New Assets**

    Question: Are new assets introduced in the paper well documented and is the documentation provided alongside the assets?

    Answer: [No]

    Guidelines:

    - The answer NA means that the paper does not release new assets.
    - Researchers should communicate the details of the dataset/code/model as part of their submissions via structured templates. This includes details about training, license, limitations, etc.
    - The paper should discuss whether and how consent was obtained from people whose asset is used.
    - At submission time, remember to anonymize your assets (if applicable). You can either create an anonymized URL or include an anonymized zip file.

14. **Crowdsourcing and Research with Human Subjects**

Question: For crowdsourcing experiments and research with human subjects, does the paper include the full text of instructions given to participants and screenshots, if applicable, as well as details about compensation (if any)?

Answer: [No]

Guidelines:

- The answer NA means that the paper does not involve crowdsourcing nor research with human subjects.
- Including this information in the supplemental material is fine, but if the main contribution of the paper involves human subjects, then as much detail as possible should be included in the main paper.
- According to the NeurIPS Code of Ethics, workers involved in data collection, curation, or other labor should be paid at least the minimum wage in the country of the data collector.

15. **Institutional Review Board (IRB) Approvals or Equivalent for Research with Human Subjects**

Question: Does the paper describe potential risks incurred by study participants, whether such risks were disclosed to the subjects, and whether Institutional Review Board (IRB) approvals (or an equivalent approval/review based on the requirements of your country or institution) were obtained?

Answer: [No]

Guidelines:

- The answer NA means that the paper does not involve crowdsourcing nor research with human subjects.
- Depending on the country in which research is conducted, IRB approval (or equivalent) may be required for any human subjects research. If you obtained IRB approval, you should clearly state this in the paper.
- We recognize that the procedures for this may vary significantly between institutions and locations, and we expect authors to adhere to the NeurIPS Code of Ethics and the guidelines for their institution.
- For initial submissions, do not include any information that would break anonymity (if applicable), such as the institution conducting the review.

6 Appendix

6.1 Proof of ST-PPR Algorithm

Theorem: Let a subgraph sampling strategy S generates a subgraph. Define structural preservation score $\rho(\mathcal{G}_s)$ as the graph kernel similarity between $\mathcal{G}_s$ and the original graph $\mathcal{G}$: $\rho(\mathcal{G}_s) = \frac{\langle \phi(\mathcal{G}), \phi(\mathcal{G}_s) \rangle}{\|\phi(\mathcal{G})\| \cdot \|\phi(\mathcal{G}_s)\|}$, where $\phi(\cdot)$ is a graph kernel mapping function. For any graph $\mathcal{G}$, there exist constants $\epsilon_1, \epsilon_2, \epsilon_3 > 0$ such that: $\rho(\mathcal{G}_{\text{integ}}) \geq \max\{\rho(\mathcal{G}_{\text{PPR}}), \rho(\mathcal{G}_{\text{BFS}}), \rho(\mathcal{G}_{\text{DFS}})\} + \epsilon_{\text{integ}}$, where ϵ_{integ} represents the gain from integration. This ensures comprehensive feature extraction including global topology , hierarchical transitions and local communities, which boosts the performance of GNNs.

Proof: PPR selects high-centrality nodes via its stationary distribution π. For any node u, its PageRank value satisfies: $\pi(u) = \alpha \sum_{v \in \mathcal{V}} \pi(v) \frac{A_{vu}}{d(v)} + (1-\alpha) q(u)$, where $d(v)$ is the degree of v, and $q(u)$ is the initial distribution. High-$\pi(u)$ nodes form the backbone of $\mathcal{G}$, ensuring $\rho(\mathcal{G}_{\text{PPR}}) \geq \epsilon_1$. For any node u, its local clustering coefficient $C(u)$ in BFS subgraph satisfies: $C_{\text{BFS}}(u) \geq C_G(u) - \delta_1$, where δ_1 bounds sampling error. Thus, $\rho(\mathcal{G}_{\text{BFS}}) \geq \epsilon_2$. DFS retains long-range dependencies. Let D be the diameter of G. The diameter of the DFS subgraph D_{DFS} satisfies: $D_{\text{DFS}} \geq D - \delta_2$, where δ_2 bounds path truncation error. Hence, $\rho(\mathcal{G}_{\text{DFS}}) \geq \epsilon_3$. The joint structural representation is: $\phi(\mathcal{G}_{\text{integ}}) = \phi(\mathcal{G}_{\text{PPR}}) \oplus \phi(\mathcal{G}_{\text{BFS}}) \oplus \phi(\mathcal{G}_{\text{DFS}})$, where $\oplus$ denotes node concatenation. By linearity of kernel functions: $\rho(\mathcal{G}_{\text{integ}}) \geq \max\{\rho(\mathcal{G}_{\text{PPR}}), \rho(\mathcal{G}_{\text{BFS}}), \rho(\mathcal{G}_{\text{DFS}})\}$. When structural information from three strategies is non-overlapping, $\epsilon_{\text{integ}} > 0$.

6.2 Algorithm of Multi-view Decomposition and Learning

Algorithm 3 Multi-view Decomposition and Learning

Input: Graph dataset $\mathbb{G} = \{(\mathcal{G}_t, y_t)\}_{t=1}^{n}$, the graph model f_{GMV}, loss weight α
Output: Trained graph model f_{GMV}

while not convergence **do**
  for src = 1 : n **do**
    $\mathcal{G}_{\text{trg}}, y_{\text{trg}} \leftarrow$ randomly sample a graph from $\mathbb{G}/\{\mathcal{G}_{\text{src}}\}$
    $\mathcal{G}_{\text{mix}}, \mathbf{E}_{\text{src}}, \mathbf{E}_{\text{trg}}, w_{\text{src}}, w_{\text{trg}} \leftarrow$ employ ST-SubMix between graph $\mathcal{G}_{\text{src}}$ and $\mathcal{G}_{\text{trg}}$ ▷ ST-SubMix 2
    $\hat{y}^1_{\text{src}}, \hat{y}^2_{\text{trg}}, \hat{y}^1_{\text{mix}}, \hat{y}^2_{\text{mix}} \leftarrow f_{\text{GMV}}(\mathcal{G}_{\text{mix}}, \mathbf{E}_{\text{src}}, \mathbf{E}_{\text{trg}})$
    $\ell_{\text{mix}} \leftarrow w_{\text{src}} \text{CE}(\hat{y}^1_{\text{mix}}, y_{\text{src}}) + w_{\text{trg}} \text{CE}(\hat{y}^2_{\text{mix}}, y_{\text{trg}})$
    $\ell_{\text{view}} \leftarrow \text{CE}(\hat{y}^1_{\text{src}}, y_{\text{src}}) + \text{CE}(\hat{y}^2_{\text{trg}}, y_{\text{trg}})$
    $\ell \leftarrow \ell_{\text{mix}} + \alpha \ell_{\text{view}}$ +R(θ)
    Update parameters of the model f_{GMV}
  end for
end while

In Algorithm 3, we generate a mixed-view and feed it into the GNNs. We then perform multi-view decomposition and predict the labels for each of the decomposed diverse views. To activate the dual sub-networks in the GNNs, we minimize both the mixing loss and the multi-view loss, thereby enhancing the multi-view representation of the GNNs.

6.3 Comparison Study

To validate the efficacy of our proposed GMV method, we conduct a series of comparison studies. As shown in Table 6a, within the GraphGPS framework, GMV outperforms baseline methods, including Vanilla and G-MIMO, on both the IMDBB and PROTEINS datasets. Furthermore, to examine its generality, we apply GMV to several mainstream GNN backbones. The results in Table 6b indicate that GMV can serve as a plug-and-play module, consistently improving the performance of GatedGCN, GINE, and NSA [55] across multiple molecular graph datasets, thereby demonstrating its broad applicability and effectiveness.

Method	IMDBB	PROTEINS
Vanilla	74.50 ±4.53	74.76 ± 3.24
Submix	75.34 ±3.68	75.21 ±1.42
G-MIMO	75.68 ±4.34	75.08 ±3.32
GMV	**76.70 ±3.22**	**75.78 ±4.13**

(a) Comparison on the GraphGPS framework.

	HIV	BBBP	BACE
GatedGCN	76.39	67.05	78.75
/w. GMV	**77.04**	**69.43**	**79.86**
GINE	76.45	67.56	77.91
/w. GMV	**77.76**	**70.30**	**78.82**
NSA [55]	-	84.0	72.0
/w. GMV	-	**85.50**	**74.1**

(b) Comparison on different backbones.

Table 6: Comparison studies evaluating the effectiveness and generality of our proposed GMV method. (a) Performance comparison against other methods on the GraphGPS framework. (b) Generality study by integrating GMV with different GNN backbones.

6.4 Ablation Study

Ablation of Mixup. From a data perspective, we compare various mixup strategies for mixed-view generation. As shown in Table 7a, GMV consistently achieves higher accuracy than other mixup methods, demonstrating its effectiveness. The full GMV enhances the ability of multi-view representation from data, model and optimization perspectives, including mixed-view generation, multi-view decomposition and multi-view learning. M-Mixup linearly interpolates graph representations to create mixed-views, making it difficult to apply multi-view decomposition and learning. S-Mixup uses a trained graph matching transformer to map the source graph to the target graph, which distorts the information of the source graph and hinders multi-view decomposition and learning. "GMV w. M-Mixup" and "GMV w. S-Mixup" only employ mixing loss to optimize dual sub-networks within GNNs. In contrast, SubMix and ST-SubMix generate mixed-views by connecting subgraphs, preserving subgraph view information, and enabling them to consider three perspectives concurrently. "GMV w. SubMix" and "GMV w. ST-SubMix" simultaneously consider mixed-view generation, multi-view decomposition and learning to enhance the performance of GNNs. Consequently, they outperform GMV with other mixup methods. SubMix focuses on semantic information, while ST-SubMix considers both structural and semantic information to create structure enhanced subgraph views, thus achieving state-of-the-art performance and generalization for GNNs.

Further Comparation with MIMO. In this section, we perform additional experiments on G-MIMO with various augmentations and observe that graph augmentations combined with ensemble learning enhance GNN performance. As shown in Table 7b, integrating G-MIMO with drop-based augmentations improves GCN accuracy on IMDBB. Different augmentations create diverse views

Method	GCN	GIN
Vanilla	72.30±2.84	71.70±3.10
M-Mixup	73.70±4.12	73.10±4.21
S-Mixup	72.50±2.20	72.80±3.82
SubMix	73.80±3.57	72.50±4.94
ST-SubMix	74.00±3.66	74.50±3.32
GMV /w. M-Mixup	72.40±2.33	74.10±3.96
GMV /w. S-Mixup	73.10±4.12	74.00±4.15
GMV /w. SubMix	75.00±4.28	74.10±3.32
GMV /w. ST-SubMix	**75.50±3.67**	**74.20±3.37**

(a) Ablation on mixup methods.

Method	Accuracy
Vanilla GCN	72.30±2.84
G-MIMO	72.70±2.53
G-MIMO w. DropNode	73.50±4.30
G-MIMO w. DropEdge	72.50±2.84
G-MIMO w. Subgraph (R)	73.40±4.15
G-MIMO w. Subgraph (PPR)	74.10±4.72
G-MIMO w. Subgraph (ST-PPR)	74.40±4.33
GMV	**75.50±3.67**

(b) Ablation on augmentation types.

Table 7: Ablation studies on the IMDB-BINARY dataset. All results are based on the GCN backbone. (a) Comparison of different mixup strategies. Our full model, "GMV /w. ST-SubMix", achieves the best performance. (b) Comparison of GMV against various augmentation techniques used in G-MIMO.

that boost performance of G-MIMO. The utilization of mixed-view generation provides richer view information, activating sub-networks in GNNs for enhanced representations. Additionally, GMV combines mixed-view generation and multi-view decomposition, enabling effective multi-view learning.

Performance vs. number of sub-networks. To assess framework scalability and efficiency, we compare GMV against G-MIMO by varying the number of sub-networks. The results in Table 8 are striking. GMV not only consistently outperforms G-MIMO, but its efficiency is such that using only two sub-networks (75.50%) already surpasses a 10-sub-network G-MIMO (75.30%). This significant performance gain stems from GMV's integrated design, which fosters more diverse and complementary predictions among the generated views, leading to stronger generalization. All results are based on a rigorous and fair comparison protocol.

Sub-nets	G-MIMO	GMV
2	72.70	**75.50**
4	74.40	**75.90**
6	74.52	**76.10**
8	74.73	**76.12**
10	75.30	**76.43**

Table 8: Performance vs. number of sub-networks on IMDB-B. GMV shows superior efficiency.

6.5 Hyperparameter Analysis

We conducted a sensitivity analysis on key hyperparameters: the feature augmentation ratio (p), the structure augmentation ratio (q), and the loss weight (α). As shown in Table 9, the results on the BACE dataset demonstrate the robustness of our model. Performance remains stable across a wide range of values for each hyperparameter, obviating the need for exhaustive or fragile tuning to achieve strong results. Notably, the optimal values fall within conventional ranges guided by prior work, reinforcing the model's stability and ease of adoption. To ensure full reproducibility, our complete source code and detailed settings will be made publicly available.

Augmentation Ratio (p)		**Structure Ratio (q)**		**Loss Weight (α)**	
Value	Accuracy	Value	Accuracy	Value	Accuracy
0.2	78.82	0.2	78.93	0.5	78.57
0.4	**79.43**	0.4	78.98	1.0	78.98
0.5	79.32	0.5	79.18	**2.0**	**79.43**
0.6	79.02	**0.6**	**79.43**		
0.8	78.72	0.8	78.34		

Table 9: Hyperparameter sensitivity analysis on the BACE dataset with a GIN backbone. The model exhibits robustness, with stable performance across a wide range of values. The best-performing setting for each hyperparameter is highlighted in **bold**.

6.6 Efficiency Study

We provide a transparent analysis of our method's computational cost, examining both the one-time preprocessing overhead and the online training efficiency.

One-Time Preprocessing Cost. Our method requires a one-time, offline preprocessing step to generate and cache views. As shown in Table 10, this cost is negligible. On the PROTEINS dataset, it amounts to less than five minutes, which is merely 0.4% of the total training time. This efficiency scales to the larger COLLAB dataset, where the 2-hour preprocessing cost is only 1.1% of the 180-hour training duration. This fixed cost is comparable to other advanced augmentation methods and is incurred only once, making it a highly practical investment.

Dataset	Graph Count	Preprocessing (Hours)	Total Training (Hours)
PROTEINS	1,113	$\sim$0.08	20
COLLAB	5,000	$\sim$2	180

Table 10: Offline preprocessing cost analysis. The one-time cost is minimal compared to the total training time (10-fold CV) on an NVIDIA 3090Ti GPU.

Online Training Overhead vs. Performance Gain. The online training phase is lightweight. Since all views are pre-computed and cached, the only overhead stems from view lookups and the forward passes for the sub-networks. Table 11 quantifies the trade-off between this training overhead and the resulting accuracy improvement over a GCN baseline. The results clearly show that for a manageable training overhead of +110-125%, our method delivers a substantial and consistent accuracy gain of approximately +9% across all datasets. This demonstrates a highly favorable and predictable return on computational investment, confirming the practical value of our approach.

Dataset	Num. Graphs	Avg. Edges	Training Overhead	Accuracy Gain
NCI1	4,110	32.3	+113%	+9.4%
PROTEINS	1,113	72.8	+120%	+8.8%
COLLAB	5,000	2,457.2	+125%	+9.0%

Table 11: Training time overhead vs. accuracy gain over a GCN baseline. A manageable increase in training time yields a significant and consistent performance improvement.

6.7 Multi-view Study

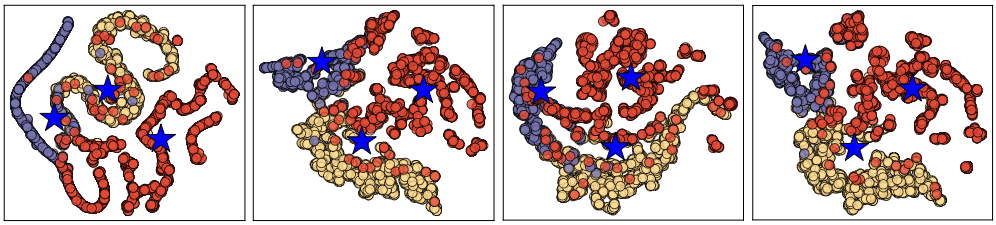

(a) 176.83 (b) 200.28 (c) 180.41 (d) 208.05

Figure 5: T-SNE among prediction outputs of vanilla GIN and GMV. (a) vanilla GIN; (b) and (c) two sub-networks within GMV; (d) GMV. The blue pentagrams denote three class center, and the digit is the distance among three class centers.

Visualization of Multi-view Representation. We employ both qualitative and quantitative methods to assess the diversity of predictions, thereby investigating the multi-view learning capacity of GMV. In Fig 5 presents the t-SNE for the vanilla GIN, two sub-networks of GIN within GMV and GMV itself, as applied to the COLLAB dataset. Different colored circles denote three classes in COLLAB, while pentagrams mark the class centers of three classes. We observe a significant difference between the two predictions, affirming the diversity of sub-networks. Moreover, the digit represents the sum of normalized l_2 distances among three centers. GMV achieves the largest distance among classes, which also validates the benefits of multi-view learning.

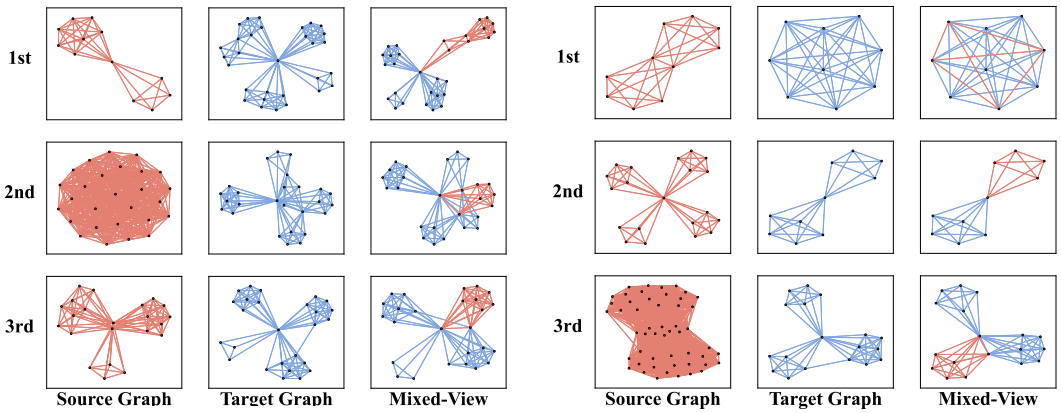

(a) IMDBB. (b) IMDBM.

Figure 6: Visualization of mixed-views on IMDBB and IMDBM.

Visualization of Mixed-view. We utilize networkx to visualize some mixed-views in Fig 6. Each row denotes the source graph, target graph and generated mixed-view. ST-SubMix consider both structure and semantic information, so it generates the subgraph views preserving the original topology structure and semantic key nodes. ST-SubMix generates diverse mixed-views for GMV to enhance multi-view representation of capacity of GNNs.

6.8 Discussion

The framework naturally extends to other crucial tasks, such as node classification and link prediction. This is achieved by leveraging the powerful paradigm of task reformulation, where local tasks are converted into graph-level problems, a strategy validated by recent work. This requires minimal architectural changes: For Node Classification: The task can be reframed as classifying a node's contextual subgraph. GMV is then applied directly to this subgraph to predict the central node's label, thereby benefiting from a robust, multi-view representation of its neighborhood. For Link Prediction: Similarly, this becomes a binary classification problem on the subgraph enclosing a pair of nodes. GMV's ability to capture diverse and subtle topological patterns makes it ideally suited for predicting the existence of a link between them. Furthermore, the core principles of GMV are adaptable to more complex domains, such as dynamic graphs (by applying the framework to temporal snapshots) and heterogeneous graphs (by acting as a modular wrapper around specialized GNN backbones).